Metallophysics and Advanced Technologies
Металофіз. новітні технол.
Metallofiz. Noveishie Tekhnol.
2021, vol. 43, No. 12, pp. 1573–1588
https://doi.org/10.15407/mfint.43.12.1573
Reprints available directly from the publisher

PHYSICS OF STRENGTH AND PLASTICITY

PACS numbers: 45.40.Gj, 81.05.Bx, 81.05.Mh, 81.40.-z

Ballistic Resistance of Layered Titanium Armour Made Using Powder Metallurgy and Additive 3D Printing

P. E. Markovsky, D. G. Savvakin, O. O. Stasiuk, S. H. Sedov[*],
V. A. Golub[*], D. V. Kovalchuk[**], and S. V. Prikhodko[***]

G. V. Kurdyumov Institute for Metal Physics N.A.S. of Ukraine,
36 Academician Vernadsky Blvd.,
03142 Kyiv, Ukraine
[*]*The National Defence University of Ukraine Named After Ivan Chernyakhovskyi,*
28 Povitroflotskyi Ave.,
UA-03049 Kyiv, Ukraine
[**]*JSC 'NVO Chervona Hvylia'*
28 Dubrovytska Str.,
UA-04114 Kyiv, Ukraine
[***]*University of California, Los-Angeles,*
CA 90095, USA

Microstructure and antiballistic protection characteristics for two types of titanium-based layered materials are studied. Binary layered armour material consisted of Ti–6Al–4V alloy and Ti–6Al–4V–10% vol. TiC metal matrix composite layers are produced using powder metallurgy and subsequent HIP treatment. Ternary Ti–6Al–4V/CP–Ti/Ti–6Al–4V armour plate is made using additive manufacturing technology. Both types of materials demonstrated a significant superiority in ballistic resistance to armor-piercing incendiary cartridges compared to uniform titanium alloys. Material microstructure and hardness, projectile penetration depth and kinetic energy are analysed to understand contribution of each layer in projectile retardation and energy dissipation. Hard front composite layer effectively retards the projectiles than softer and ductile Ti–6Al–4V and CP–Ti layers, while combination of these materials ensures lower penetration depth and absence of armour cracking on high-energy ballistic impact.

Corresponding author: Dmytro Georgiyovych Savvakin
E-mail: savva@imp.kiev.ua

Citation: P. E. Markovsky, D. G. Savvakin, O. O. Stasiuk, S. H. Sedov, V. A. Golub, D. V. Kovalchuk, and S. V. Prikhodko, Ballistic Resistance of Layered Titanium Armour Made Using Powder Metallurgy and Additive 3D Printing, *Metallofiz. Noveishie Tekhnol.*, **43**, No. 12: 1573–1588 (2021), DOI: 10.15407/mfint.43.12.1573.

Key words: titanium alloys, metal matrix composites, layered materials, ballistic resistance, titanium armour, powder metallurgy, additive manufacturing, hot isostatic pressing.

Досліджено мікроструктуру та антибалістичні захисні характеристики двох типів шаруватих титанових матеріалів. Двошарові броньовані пластини, що складалися зі стопу Ti–6Al–4V та металоматричного композиту Ti–6Al–4V–10% об. TiC одержано методом порошкової металургії з використанням гарячого ізостатичного пресування. Потрійні пластини Ti–6Al–4V/CP–Ti/Ti–6Al–4V виготовлено за адитивними технологіями (3D друку). Обидва типи шаруватих матеріалів показали перевагу в антибалістичному захисті порівняно з однорідними титановими стопами під час випробувань бронебійними уражальними елементами. Проаналізовано мікроструктуру та твердість окремих шарів, глибину проникнення та кінетичну енергію куль, що дало змогу зрозуміти вклад кожного шару в затримку куль та дисипацію їхньої енергії. Твердий передній шар металоматричного композиту ефективніше зупиняє уражальні елементи, ніж м'які та пластичні шари стопу Ti–6Al–4V та технічно чистого титану, а комбінація цих матеріалів забезпечує зменшення глибини проникнення та відсутність розтріскування шаруватих структур у разі балістичного удару.

Ключові слова: титанові стопи, металоматричні композити, шаруваті структури, антибалістичний опір, титанова броня, порошкова металургія, адитивні технології, гаряче ізостатичне пресування.

(Received September 30, 2021)

1. INTRODUCTION

High specific strength and corrosion resistance of Ti-based alloys make them well-established and highly requested materials for aerospace, chemical, medical and others industrial applications, including military, in particular for armoured protecting elements [1–3]. However, sometimes the set of noted characteristics is insufficient for the extreme requirements of reliable protection against ballistic impact of various shells, despite the attractive combination of high strength, ductility and toughness of titanium materials. Besides, the low wear resistance of titanium alloys limits their practical use. The desired combination of mechanical characteristics can be achieved using laminates that combine two or more layers having different chemical composition and/or microstructure, and therefore can have different mechanical properties within each individual layer providing unique characteristics of the entire part. Thus, the objectives of the layered structures fabrication are to provide materials that have service characteristics unattainable for homogeneous structures. For example, laminates composed of various titanium alloys and metal matrix com-

posites (MMC) on their base are characterized by an improved combination of mechanical characteristics owing to high ductility and toughness of alloy layers and the increased strength and hardness of the MMC, resulting in device properties unachievable for the alloy or composite standing alone.

As previously shown [4–6], blended elemental powder metallurgy (BEPM) using the simplest form of pressing and sintering allows cost-efficient manufacturing of laminates consisting of Ti–6Al–4V alloy and MMC's based on it, reinforced with particles TiB and TiC. Fabrication of said multi-layered structures is not possible by conventional cast and wrought metallurgy. In contrast, the correct selection of BEPM processing parameters ensures the desired microstructure within each layer and sufficient bonding between the layers of the different compositions, which, in turn, fosters the mechanical characteristics of laminates. Layered armour plates with sufficient mechanical and protective characteristics are successfully manufactured as a result of purposeful adjustment of BEPM processing parameters [4–5]. Though, sintered materials depending on their compositions usually contained 3–8% residual porosity, which can compromise their performance. It is discussed [7] that a further improvement of mechanical and antiballistic protecting characteristics is highly possible via reduction of residual porosity. The post-sintering hot deformation is traditionally considered as the most common way of this defect correction. Nevertheless, its application for laminates' treatment is found to be limited [7]. That is why a few different ways of bonding individually fabricated by BEPM layers into laminate are suggested, namely diffusion bonding, friction welding and hot isostatic pressing (HIP). The feasibility of the first two has already been discussed in previous publications [8, 9] whereas the HIP followed the BEPM processing will be given more attention in present communication. The HIP process combines high temperature and high pressure inside the HIP reaction chamber, which allows solid-phase consolidation of powders to a completely dense structure of fine grains, as well as diffusion bonding of solid and porous parts [10].

At the same time, additive manufacturing (AM), also known as 3D printing, is transformative technology [11, 12] using local melting of powder bath or wire are also very promising for layered structures fabrication, allowing combination of different materials with different properties into integrated device. The correct selection of AM parameters can ensure formation of poreless structures with controllable grain size that provide the improved mechanical characteristics.

The purpose of the present study is to identify the potential of the two methods noted: (i) HIP in combination with BEPM and (ii) AM for the manufacturing of titanium-based laminates with projected low-porosity microstructures and a set of mechanical characteristics suffi-

cient for practical use as armour elements, and to show their position among materials currently proposed by the relevant industry.

2. EXPERIMENTAL PROCEDURE

The present study used two different ways of making laminates shown in Fig. 1. Double-layer plates consisting of Ti–6Al–4V (wt.%) alloy (Ti-64) and MMC based on it, reinforced with particles TiC (10% vol.) are made using BEPM followed by HIP. The three-layer plates consisted of the outer Ti-64 layers and the inner CP–Ti layer between them are made using AM. The BEPM fabrication used hydrogenated titanium (TiH_2) powder. It has been shown that the hydrogen involvement as a temporary alloying element in the sintering process has a very beneficial effect on the activation of sintering and purification of the alloy [13]. Two different TiH_2 powder sizes, fine, less than 100 μm and coarse, 100–125 μm, are used to prepare the blends. A master alloy powder 60Al–40V less than 63 μm in size is added to TiH_2 to form the alloy composition Ti-64. A powder TiC 1–30 μm in size is further added to create the MMC blend. Individual powder blends are die compacted at 150 MPa at the room temperature to form the plates powder preforms with dimension 90×90×12 mm. Then preforms are sintered in vacuum at 1250°C for 4 h for their dehydrogenation and complete consolidation to produce the plates of the alloy and composite.

Cold pressed and sintered Ti-64 alloy and MMC plates produced using the same TiH_2 powder size are joined together with diffusion bonding and simultaneously densified by HIP treatment at 100 MPa and 900°C for 2 hours. The final product of this treatment is double-layer plates about 22 mm thick (Fig. 1, *a*). The noted two sizes of TiH_2 powder are used to form consolidated plates with two distinctively different porosity fractions. This is done to determine the effect of porosity and optimize its fraction on bonding quality. It is generally accepted that relatively high as-sintered porosity facilitates bonding by activating plastic deformation within the compact during HIP treatment [14].

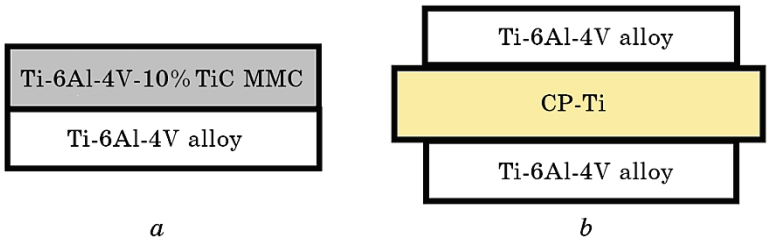

Fig. 1. Diagrams of the layered armour plates made with BEPM and HIP (*a*), AM (*b*).

The three-layer plates (Fig. 1, *b*) are fabricated using advanced AM, Direct Energy Deposition (DED), also called xBeam 3D Metal Printing [15]. The distinctive key feature of used process is the application of the hollow conical electron beam generated by low-voltage (< 20 kV) gas-discharge gun for heating and melting of the substrate and wire. It ensures precisely controllable liquid metal transfer from the wire end to the substrate, specific temperature gradients at the fusion area and heat flow from liquid metal pool. Such conditions of heating, melting and cooling during deposition of molten additive material provide controllable microstructure formation, including grain size and material texture. In AM process Ti–6Al–4V alloy wire is used as a feedstock material, while ready cast and wrought CP–Ti plate (200×250×10 mm) is used as substrate. The Ti-64 alloy layers are deposed on both sides of CP–Ti plate to form a ternary structure with a total thickness of 27 mm. Manufactured 3-layered plate is annealed at 650°C, for 4 h to reduce the structure stresses from the AM processing.

Manufactured plates are ballistically tested in the research laboratory of weapons and special protective materials of The National Defence University of Ukraine named after Ivan Chernyakhovskyi, certified according to DSTU ISO/IEC 17025:2006. The test is carried out using a ballistic barrel SVD S-08 and live ammunitions BZ and B32 armour-piercing incendiary bullets of 7.62 mm calibre with an ogival shape in a copper jacket with a steel thermally reinforced core (hardness 70 HRC). Shooting is carried out from a distance of 10 m; the speed of the bullets is measured by the optoelectronic device IBKh-731/2. The different mass and velocity of bullets provided their different kinetic energy.

The structure of the samples in the initial state and after ballistic test is characterized using light optical microscopy (LOM, Olympus IX70) and scanning electron microscopy (SEM, VEGA 3 Tescan). SEM imaging in secondary and backscattered electron mode is conducted using accelerating voltage 20 kV. The Vickers's hardness of each layer is measured using Wolpert 425 system.

3. RESULTS AND DISCUSSION

3.1. Structure of Samples before Ballistic Test

3.1.1. BEPM and HIP Fabricated Dual Layer Samples

As a result of sintering and dehydrogenation, the blend of TiH_2 and master alloy is transformed into consolidated alloy Ti-64 with homogeneous microstructure. The residual porosity depended on the size of TiH_2 powder used. The coarse base TiH_2 powder resulted in noticeably higher porosity of the alloy, which is measured as 5–7% vol., while for

the finer powder samples it is about 3–4% (Fig. 2, *a*). Porosity measured on sintered MMC samples reinforced with TiC showed the same dependence on the size of the TiH_2 powder (Fig. 2, *b*). Minor inhomogeneity is observed in the distribution of particles TiC over the alloy matrix, which is result of relatively coarse TiH_2 particles surrounded with fine TiC during initial powder blending. It is expected that the particles TiC did not substantially transform during sintering under the conditions used, but small reaction layers between the TiC and the alloy matrix are formed due to carbon diffusion [16].

The HIP treatment after sintering provided a complete connection between the plates of alloy and MMC, and sufficient porosity reduction is observed for both layers (Fig. 3). Materials that had low porosity after sintering are converted to an almost non-porous alloy and MMC (Plate No. 1, Fig. 3, *a*, *b*), while sintered materials with relatively high porosity showed no more than 2–3% of the pores after HIP (Plate No. 2, Fig. 3, *c*). HIP procedure has resulted in high-quality integration between the alloy and MMC layers without excessive porosity and cracking in the interfaces (Fig. 3, *d*).

The measured hardness of sintered materials shows a marked variation in values due to the presence of pores, as well as due to not very uniform distribution of reinforcing TiC particles in the MMC. For sintered samples, Vickers's hardness values ranged within 295–315 HV for the alloy Ti-64 and 350–375 HV for the MMC depending on structures' porosity. Decrease in porosity after the HIP resulted in increased hardness of the alloy and composite.

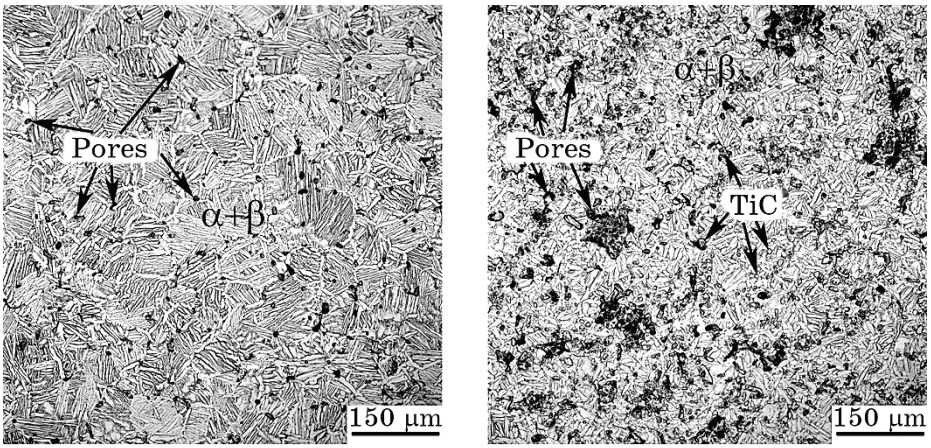

a *b*

Fig. 2. Typical microstructure (LOM) of low initial porosity samples after sintering: alloy, Ti-64 (*a*) and MMC, Ti-64 + 10TiC (*b*).

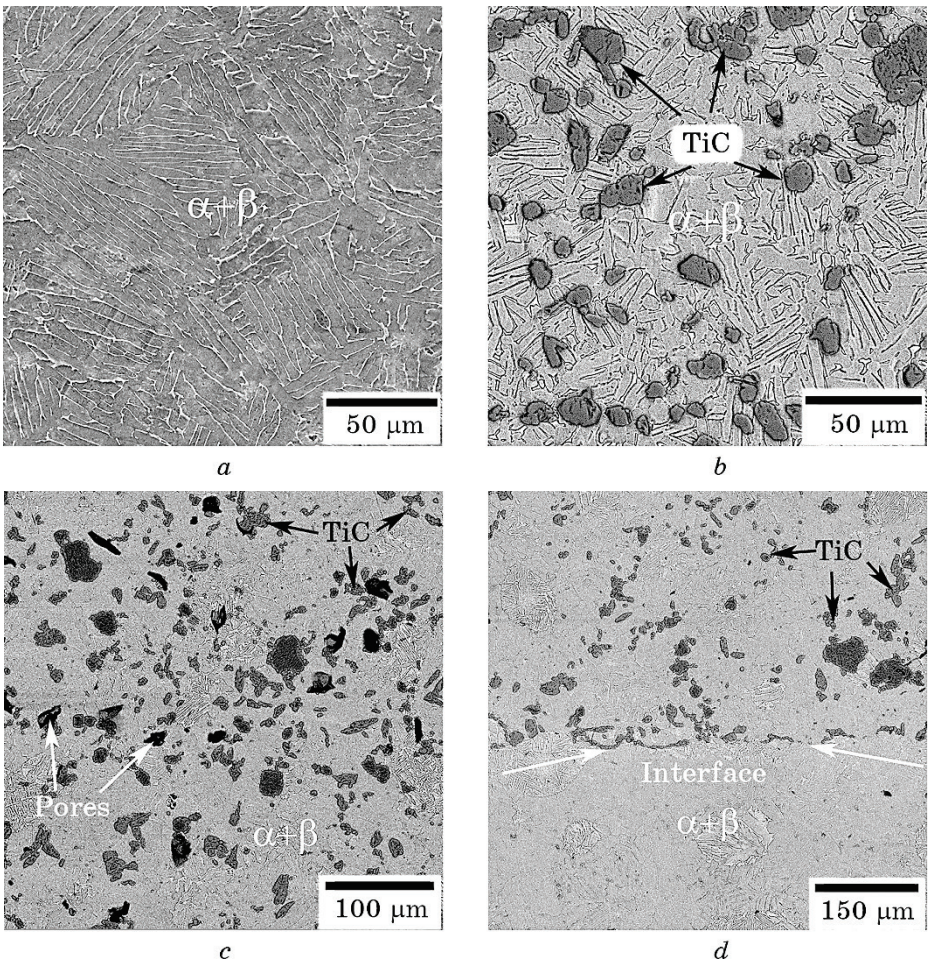

Fig. 3. SEM images of binary plates after BEPM and HIP fabrication. Plate No. 1: structure with low as-sintered porosity transforms after HIP to a nearly non-porous alloy (*a*) and MMC (*b*). Plate No. 2: MMC with increased as-sintered porosity preserved residual pores after HIP (*c*) and interface between MMC and Ti–6Al–4V layers (*d*).

The hardness of non-porous alloy is average measured 325 HV, while MMC is 385 HV. The increase in hardness is also measured on initially (as-sintered condition) high porous materials after their additional HIP treatment, which did not completely eliminate porosity but significantly reduced it, providing 329 HV for the alloy and 407 HV for the MMC. Such result is unexpected, however, can be explained with more manifested oxygen 'pick up' of highly porous plates upon HIP process.

3.1.2. AM Fabricated Three-Layer Plate

Microstructure of three-layer plate fabricated using AM is shown in Fig. 4 in vicinity of the interface between Ti-64 and CP–Ti layers. The interfaces between the core plate of CP–Ti and the AM-deposited layers of Ti-64 alloy demonstrate a high quality fusion indicating of successful bonding of the layers without visible defects and pores (Fig. 4). The CP–Ti layer represents a fine-grain globular structure. The Ti-64 layers formed as a result of deposition and crystallization during AM process demonstrate relatively coarse, mainly columnar-like grains with fine lamellar $\alpha + \beta$ intragrain microstructure formed during post processing cooling and subsequent annealing. The measured hardness of CP–Ti layer is188 HV. The hardness of Ti-64 layers on both sides of CP–Ti is noticeably higher and measured at 345 HV.

3.2. BALLISTIC TESTS RESULTS

3.2.1. Binary-Layered Ti-64 // Ti-64 + 10TiC Armour Plates Made Using BEPM and HIP

The general view of the plates after the ballistic test is shown in Fig. 5. Test data, measured and calculated parameters including kinetic energy of bullets are given in Table 1. It is accepted that the kinetic energy of projectile upon its penetration through the target is dissipated during the ballistic impact due to the deformation of the target material. The volume of deformed material depends on the projectile caliber. The projectile penetration ability is most conveniently reflected by the specific kinetic energy (SKE) calculated as the kinetic energy of the pro-

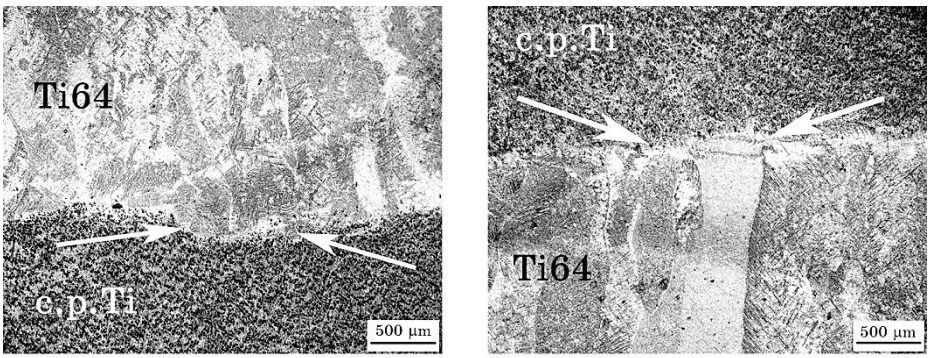

a *b*

Fig. 4. LOM images of the structures of the interface area (arrowed) between the CP–Ti substrate and the Ti-64 alloy layers AM-built in the upper portion (*a*), and in the lower portion of the substrate (*b*).

jectile divided on the cross section of the hole made by the projectile in material.

It is also listed in Table 1 and has been used to compare current results with previously published data for other alloys used for armour. The binary plates No. 1 and No. 2 are ballistically tested with the projectile impacted on the front hard MMC side (Fig. 5, *a*, *b*). Both tested binary plates did not show signs of piercing on the back side. However, the MMC and the alloy layers detached during the test on plate No. 1, which is made of initially low porous materials. This confirms a higher efficiency of HIP joining when materials have relatively higher porosity initially, before the processing. For the both tested samples, the projectiles stopped within the hard front MMC layer. The bullet penetration depth measured is about 10 mm (Fig. 6, *a*) and no visible deformation of the back side of the laminate plate is observed. The copper jacket and the lead filling of the bullet are detached from the solid core at the very top of the crater (indicated with I) and the crater is not exactly perpendicular to the plate surface.

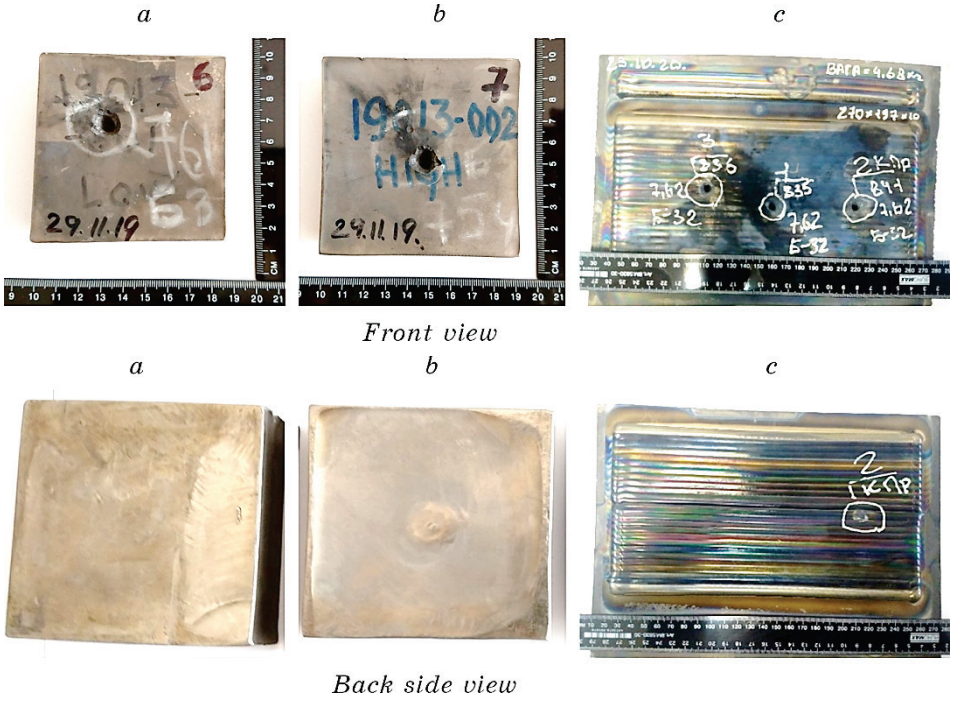

Fig. 5. Armour plates view after ballistic test. Binary Ti-64 // Ti-64 + 10TiC plates manufactured using BEPM and HIP are shown in two left columns: plate No. 1 of low-porosity (*a*), plate No. 2 of high-porosity (*b*), ternary armour plate Ti-64 // CP–Ti // Ti-64 AM-made (*c*).

TABLE 1. Armour plates ballistic test results.

No.	Description of the test outcome	Projectile penetration depth, mm	Bullet type and Kinetic energy, J	SKE, J/mm^2
	Binary armour: Ti-64 + 10TiC // Ti-64, BEPM and HIP made, low porosity			
1	Not pierced; MMC and alloy layers are detached	10 inside of MMC	BZ, 2143	47.0
	Binary armour: Ti–6Al–4V–10TiC/Ti–6Al–4V BEPM and HIP made, high porosity			
2	Not pierced; MMC and alloy layers are not detached	9.8 inside of MMC	BZ, 2104	46.1
	Ternary armour Ti-64 // CP–Ti // Ti-64 AM-made			
3	Partially pierced; projectile stuck in the plate	27 Penetration through 3 layers	B32, 3678	80.7
4	Not pierced	22 Stopped within back layer	B32, 3634	79.7
5	Not pierced	19 Stopped within back layer	B32, 3626	79.5

The penetration of the projectile through the MMC layer is accompanied by its noticeable local deformation and the formation of adiabatic share bands (ASB) shown in Figs. 6, *b*, *c*. Severe plastic deformation of the soft Ti-64 matrix alloy with fragmentation of α-lamellae occurred inside the ASB, with no visible fragmentation of hard particles TiC (Fig. 6, *d*). As can be seen in Fig. 6, *c* the severe deformation of metal matrix around coarse TiC particles resulted in cracks formation within the ASB.

3.2.2. Ternary Armour Plates Ti-64 // CP–Ti // Ti-64 AM Fabricated

The structure of ternary plates AM-made after ballistic tests are shown in Fig. 7. For all bullet speeds tests the projectiles pierced the front Ti-64 and the core CP–Ti layers and then stopped within the back Ti-64 layer (Nos. 3–5, Table 1). Presented results provided a unique opportunity to assess the threshold kinetic energy of the projectile needed to pierce this particular structure.

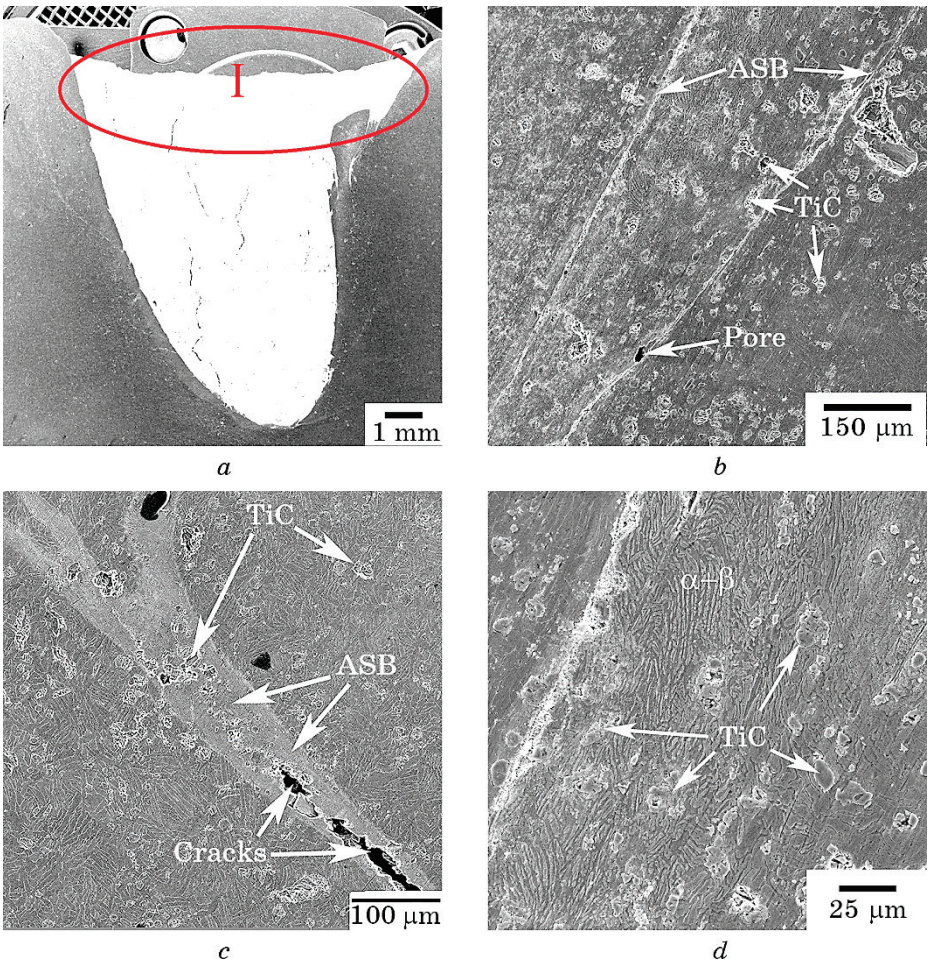

Fig. 6. Microstructure of two-layered armour Ti-64 + 10% TiC // Ti64 front layer after ballistic test in vicinity of the impact: general view (*a*), ASB (*b*, *c*), and deformed α + β matrix with TiC particles within the ASB (*d*).

A clear and gradual relationship is found between the velocity of the bullet (and therefore their kinetic energy) and the depth of penetration (Fig. 8). The depth of penetration is 22 mm and 19 mm for two projectiles (Fig. 7, *a*, Table 1, Nos. 4, 5), at the same time the higher velocity projectile is stopped with partial piercing and destruction of the back surface (Fig. 7, *e*, Table 1, No. 3). The bonding between layers is not disrupted for all cases (Fig. 7, *b*), but it should be noted that, stronger Ti-64 alloy is imbedded into the softer CP–Ti layer in the deformed area near the bullet channel (Fig. 7, *b*). The uneven surface (dimples) on the reverse side of the plate, formed at the joints between the molted

areas during AM processing, acted as a stress concentrator, which led to the crack formation even in the case of incomplete penetration of the 3-layer plate (Fig. 7, *c*). A severely deformed area near the projectile tip is observed. It shows a network of interconnected ASBs and some of them developed into cracks (Fig. 7, *d*).

A similar microstructure is observed along the channel in the case of the highest bullet velocity and the deepest bullet penetration into the plate (Fig. 7, *e*), including the formation of a large number of ASB and lateral cracks extending from them (Fig. 7, *f*). A large number of small

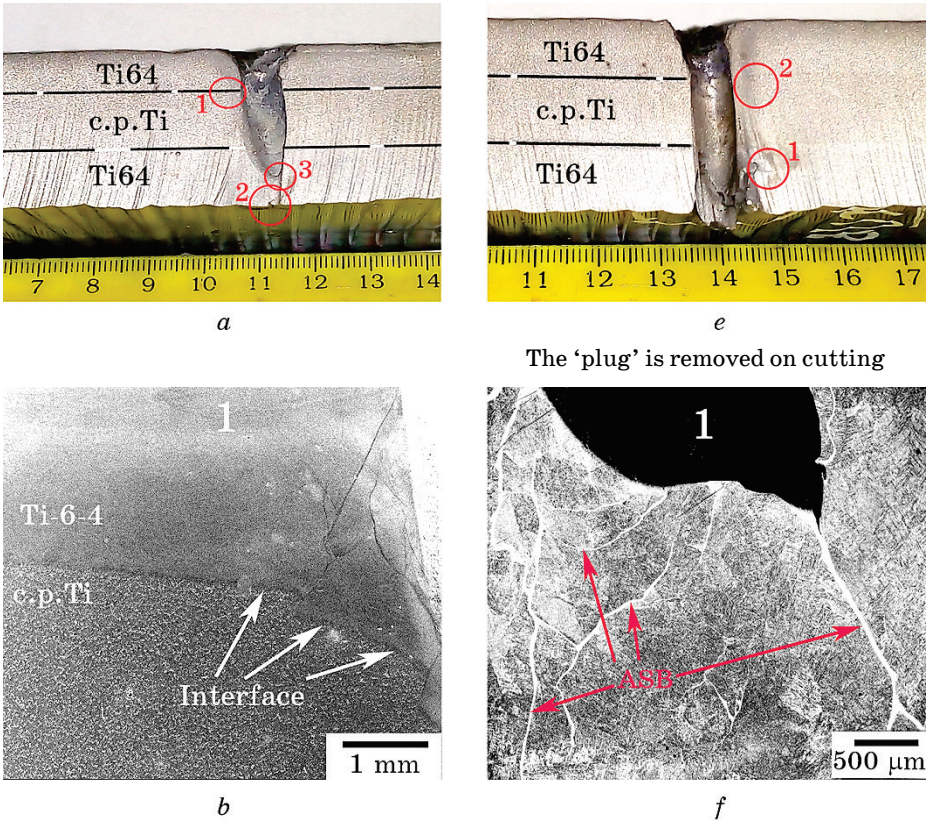

Fig. 7. The SEM view of ternary plate AM-made after ballistic tests: after the shot with bullet SKE 76.5 J/mm^2 (No. 5, Table 1) (*a*–*d*) and 80.7 J/mm^2 (No. 3, Table 1) (*e*–*h*), the interface between the front Ti-64 and the core CP–Ti layers (*b*); the crack initiated on the back side by surface relief formed during AM fabrication (indicated by red circle) (*c*); ASBs formed in Ti-64 layer under the pierced channel (*d*); crack initiation at the ABS (*f*); severely deformed Ti-64 layer with the cracks (*g*, *h*). The numbers in the top of (*b*), (*c*), and (*d*) correspond to the areas indicated by the circles in (*a*); the same in the top of (*f*), (*g*), and (*h*) correspond to areas indicated by circles in (*e*).

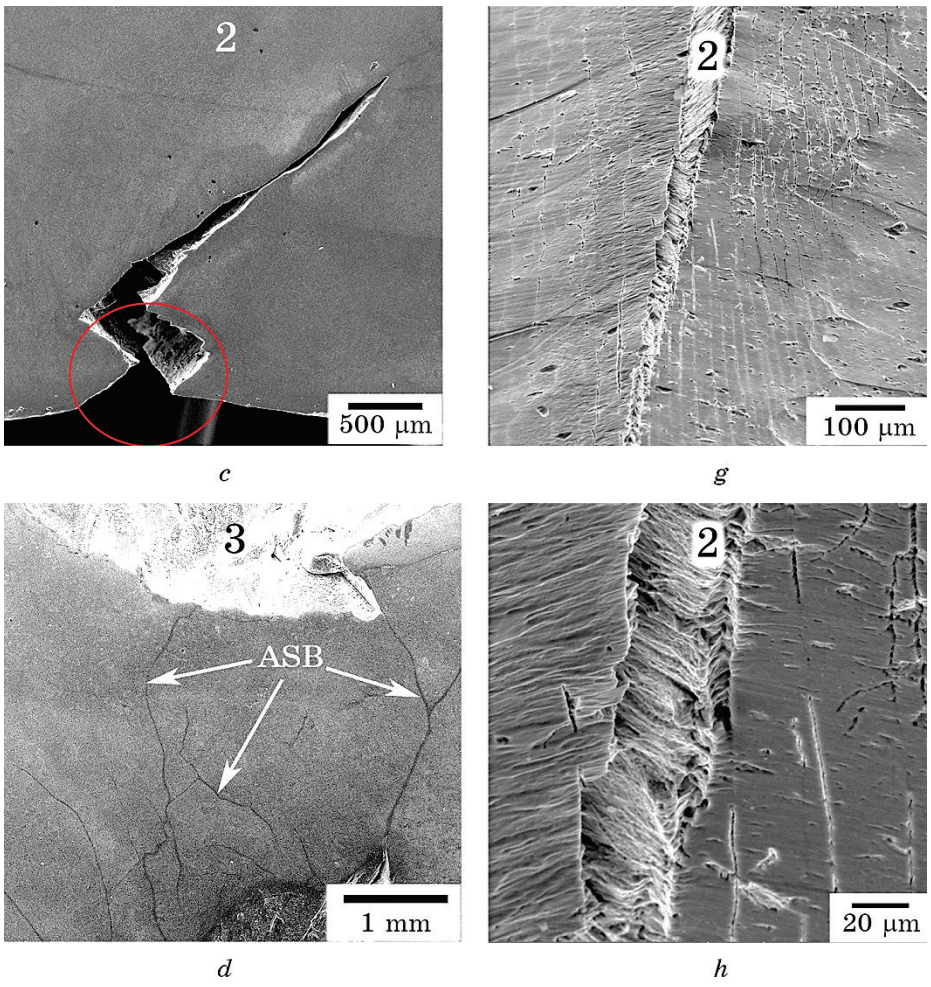

Continuation of Fig. 7.

parallel cracks are observed in the deformed area between the coarse primary cracks (Fig. 7, *g*). The fracture surfaces mainly indicated a ductile mode, demonstrating a good margin of plasticity in the 3D printed materials (Fig. 7, *h*).

The ballistic test results are summarized in Fig. 8 together with previously published data on various homogeneous titanium alloys. The SKE of the projectile and the depth of its penetration (Table 1, Fig. 8) are the key parameters in assessing the ability to dissipate the energy of the projectile by various armour materials, which allows to determine the thickness of the armour that provides full protection. It should be emphasized that the resistance of both binary BEPM-made and triple AM-made materials to both types of armour-piercing incen-

diary cartridges significantly exceeds such characteristics for the previously studied uniform Ti-64 and T110 titanium alloys (*1* and *2* in Fig. 8 [2], [17]).

To summarize, armour made using BEPM and HIP route can provide sufficient protective characteristics under the conditions studied, when a hard layer of MMC of about 10 mm thick is placed as a front layer of laminated armour, which avoids piercing (Fig. 8). Due to the projectiles are stopped within MMC layer, the average resistance force F of the MMC material on projectile penetration is calculated following the equation $F = E_{kin}/d$, where E_{kin} is the projectile SKE and d is depth of penetration. The F is measured as $(4.6–4.8)\cdot10^9$ N. At the same time, the role of the back side plastic Ti-64 alloy layer for such binary armour plates is very important to prevent the possible cracking of MMC. Most likely, the MMC layer alone of similar thickness (~11 mm) could not stop the projectiles due to brittle fracture. It is also apparent that the interface between the layers also contributes to the projectile retardation, since the interlayer surfaces contribute to the additional dissipation of ballistic impact energy with the bounce of shock waves in direction along the interface [18].

Ternary armour plates produced with AM demonstrate noticeably deeper penetration of the projectiles because the Ti-64 and, especially, core CP–Ti layers are markedly softer compared to MMC [19]. Moreo-

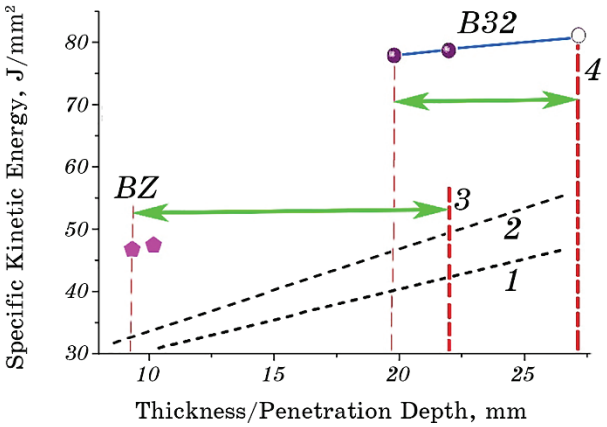

Fig. 8. Results of ballistic tests in SKE of projectile *vs* thickness of tested plates/bullet penetration depth coordinates *1* and *2* are earlier published data on Ti-64 [2] and T110 [17] alloys, respectively, fabricated using conventional cast and wrought metallurgical approach; *3*—thickness of BEPM plates Nos. 1, 2; *4*—thickness of the triple Ti-64/CP–Ti/Ti-64 AM plate. Closed symbols—not pierced, open symbol—pierced cases showing projectiles penetration depth. Horizontal arrows indicate possible reserve for reduction of armour materials thickness.

ver, higher kinetic energy of B32 contributes to deeper penetration. Analysis of SKE of B32 projectiles and the depth of penetration for 3 shoots (Table 1, Fig. 8) reveals that the average resistance force F for ternary layered material is within $3.0–4.2 \cdot 10^9$ N, *i.e.* lower compared to MMC.

It can be concluded from Fig. 8 results, that both types of tested layered materials demonstrated improved protecting characteristics against high-energy and hard core BZ and B32 projectiles compared to corresponding characteristics of uniform titanium alloys Ti-64 and T110. Noticeable difference between the projectile depth of penetration and the total thickness of tested layered plates (arrowed in Fig. 8) presents an opportunity for further thickness reduction of the armour plates. The most promising in this regard looks the thickness reduction of the ductile back Ti-64 layer in binary plates BEPM and HIP made, leaving the thickness of the front MMC layer unchanged.

4. CONCLUSIONS

1. Two innovative and cost-efficient approaches: (i) BEPM followed the HIP and (ii) AM are used for the successful fabrication of titanium-based laminates.
2. The binary MMC/Ti64, BEPM and HIP-made and ternary Ti-64/CP–Ti/Ti-64, AM-made armour plates have a significant superiority in ballistic resistance to armour-piercing incendiary cartridges compared to armour made of uniform titanium alloys Ti-64 and T110.
3. Analysis of material microstructure and hardness, projectile penetration depth and kinetic energy promoting understanding of contribution of each material in projectile retardation and energy dissipation. Difference between projectile penetration depth and total thickness of tested layered plates gives an opportunity for thickness reduction of tested armour materials, first of all, owing to using thinner ductile back layer.

ACKNOWLEDGMENTS

Part of the work related to the manufacture and study of two-layer plates by the BEPM method is carried out at the expense of the NATO project G5787 within the framework of the ‘Science for Peace and Security’ program. Ballistic tests are carried out within the framework of the Agreement on Scientific and Technical Cooperation between the G. V. Kurdyumov Institute for Metal Physics of N.A.S. of Ukraine and The National Defence University of Ukraine named after Ivan Chernyakhovskyi.

Authors would like to acknowledge Dr. Victor Samarov (Synertech PM, USA) for HIP treatment of the samples.

REFERENCES

1. G. Luetjering and J. C. Williams, *Titanium* (Berlin: Springer: 2007).
2. J. Fanning, *J. Mater. Eng. Perform.*, **14**: 686 (2005).
3. J. S. Montgomery and M. G. Y. Wells, *JOM*, No. 4: 29 (2001).
4. P. E. Markovsky, D. G. Savvakin, O. M. Ivasishin, V. I. Bondarchuk, and S. V. Prikhodko, *J. Mater. Eng. Perform.*, **28**, Iss. 9: 5772 (2019).
5. O. M. Ivasishin, P. E. Markovsky, D. G. Savvakin, O. O. Stasiuk, M. Norouzi Rad, and S. V. Prikhodko, *J. Mater. Processing Technol.*, **269**: 172 (2019).
6. O. M. Ivasishin, P. E. Markovsky, D. G. Savvakin, O. O. Stasiuk, V. A. Golub, V. I. Mirnenko, S. H. Sedov, V. A. Kurban, and, S. L. Antonyuk, *Usp. Fiz. Met.*, **20**, No. 2: 285 (2019).
7. S. Prikhodko, P. Markovsky, D. Savvakin, O. Stasiuk, and O. Ivasishin, *Mater. Sci. Forum*, **941**: 1384 (2018).
8. S. V. Prikhodko, D. G. Savvakin, P. E. Markovsky, O. O. Stasuk, J. Penney, A. A. Shirzadi, P. D. Davies, and H. M. Davies, *Sci. Technol. Welding Joining*, **25**, Iss. 6: 518 (2020).
9. S. V. Prikhodko, D. G. Savvakin, P. E. Markovsky, O. O. Stasuk, J. Penney, N. Enzingen, M. Gaskil, and F. Deley, *Welding in the World*, **65**: 415 (2021).
10. V. Samarov, *PMTi 2019: Powder Metallurgy and Additive Manufacturing of Titanium Conference (Sept. 24-27, 2019)* (Salt Lake City, Utah: University of Utah).
11. W. E. Frazier, *J. Mater. Eng. Perform.*, **23**, No. 6: 1917 (2014).
12. Shunyu Liu and Yung C. Shin, *Materials and Design*, **164**: 107552 (2019).
13. O. M. Ivasishin and V. S. Moxson, *Titanium Powder Metallurgy. Science, Technology and Applications* (Eds. Ma Qian and F. H. Froes) (Elsevier: 2015), p. 117.
14. H.-xing Wang, Yan Zhang, Sh.-feng Yang, and B.-yi Liu, *Trans. Nonferrous Met. Soc. China*, **24**, Iss. 2: 449.
15. D. Kovalchuk, V. Melnyk, I. Melnyk, D. Savvakin, O. Dekhtyar, O. Stasiuk, and P. Markovsky, *J. Mater. Eng. Perform.*, **30(7)**: 5307 (2021).
16. P. Wanjara, P. A. L.Drew, J. Root, and S. Yue, *Acta Mater.*, **48**, Iss. 7: 1443 (2000).
17. P. E. Markovsky, V. I. Bondarchuk, S. V. Akhonin, and A. V. Berezos, *Proceedings of 14th World Conference on Ti (10–15 June, 2019, Nantes, France)* MATEC Web of Conferences, **321**, 11036 (2020).
18. J. K. Lee, *Analysis of Multi-Layered Materials under High Velocity Impact Using CTH* (Thesis of Disser. for Master Sci. in Aeronautical Engineering), 2685 (2008).
19. P. E. Markovsky, D. G. Savvakin, S. V. Prikhodko, O. O. Stasyuk, S. H. Sedov, V. A. Golub, V. A. Kurban, and E. V. Stecenko, *Metallofiz. Noveishie Technol.*, **42**, No. 11: 1509 (2020).